Available online at www.sciencedirect.com

ScienceDirect

Energy Procedia 92 (2016) 743 – 749

Energy Procedia

6th International Conference on Silicon Photovoltaics, SiliconPV 2016

Impact of Ag pads on the series resistance of PERC solar cells

Henning Schulte-Huxel[a,*], Robert Witteck[a], Paula van Laak[a], Till Brendemühl[a], David Hinken[a], Karsten Bothe[a], and Rolf Brendel[a,b]

[a]*Institute for Solar Energy Research Hamelin (ISFH), Am Ohrberg 1, D-31860 Emmerthal, Germany*
[b]*Dep. Solar Energy, Inst. Solid-State Physics, Leibniz University of Hannover, Appelstr. 2, 30167 Hanover, Germany*

Abstract

Screen-printed passivated emitter and rear cells (PERC) require Ag pads on the rear side to enable solderable connections for module integration. These Ag pads are separated from the silicon by a dielectric layer to avoid recombination of minority charge carriers. The drawback of this configuration is an elongated transport path for the majority charge carriers generated above the pads. This results in an increase in series resistance. The strength of this effect depends on charge carrier generation above the Ag pads that critically depends on shading of the cell's front side. Ag pads are usually wider than the busbars or the interconnector ribbons and thus are only partially shaded. We build PERC test structures with various rear side configurations of Ag and Al screen printing as well as with and without laser contact openings (LCO). Using experiments and finite element simulations we investigate the impact of shading the Ag pads by the busbars and other means. While fully shaded regions do not increase the lumped solar cell's series resistance, unshaded Ag pads lead to an increase of about 37%.

Peer review by the scientific conference committee of SiliconPV 2016 under responsibility of PSE AG.

Keywords: PERC solar cells; module interconnection; laser fiered contacts; laser welding

1. Introduction

The standard interconnection technique for industrial screen-printed crystalline Si solar cells is soldering [1]. However, soldering requires a solderable cell metallization, like silver or copper, since Al is not solderable with the standard processes used in the PV industry [2]. The front side metallization of screen-printed PERC solar cells is made out of silver. On the rear side Al screen printing is used to enable the formation of a local Al back surface field

* Corresponding author. Tel.: +49-5151-999-303; fax: +49-5151-999-400.
E-mail address: h.schulte-huxel@isfh.de

Peer review by the scientific conference committee of SiliconPV 2016 under responsibility of PSE AG.
doi:10.1016/j.egypro.2016.07.053

(BSF). To enable soldering on the rear side Ag or Ag-Al metallizations are applied locally. These regions are called solder or Ag pads. Comparing the solder pads of various commercial cell manufacturers we find pad widths from 2.5 to 4 mm. They are thus considerably wider than the front side busbars, which are typically 0.5 mm for solar cells with five busbars and 1.2 mm for three busbar cells. The pads are also wider than the interconnector ribbons that measure 0.8 to 2 mm in width. The reason for the pads being wider than the ribbons is to allow some alignment tolerance for the tabber-stringer tool. In case of cells without dielectric rear side passivation layer, the Ag pads suppress the formation of an Al BSF. This leads to an increased recombination and reduces the cell efficiency by 0.1-0.4%$_{abs}$. [3,4]. In case of PERC solar cells, the pads are printed on the dielectric passivation stack so that this decrease is not expected [5] and no contact to the Si is formed. However, majority charge carriers generated above the solder pads have an elongated transport path. This causes an increased series resistance, similarly to the effects observed above the emitter busbar in back contacted solar cells [6]. Here, we investigate the series resistance effects by the solder pads and its dependence on the width of the pad and the shading of the pad.

2. Experimental investigations of PERC cells with Ag solder pads

We have to differentiate between two effects, first a possible increase in recombination in the area of the Ag pads and second an elongated majority charge carrier transport. For this reason we process five groups (1-5) of PERC solar cells [7] on 2.3 Ωcm p-type wafers. All cells feature four 1 mm-wide busbars. The rear side is passivated by 5 nm AlO_x and 100 nm SiN_x. LCOs are formed only in those regions that will later be covered by Al, i.e., not in the regions of the pads. For *I*-*V*-testing the front side busbar is contacted by contact bars, which are 2.7 mm wide. In order to quantify the impact of the pads on the cell *I*-*V*-parameters in more detail and to omit shading effects, we fabricate different solar cells, where the pads (3.2 × 7.2 mm²) are placed between the front busbars. The groups of cells featuring different combinations of screen printing and laser contact openings (LCO) in the pad regions are:

1. Al/LCO: The cells have Al screen printing and LCOs on the full rear side, i.e. also in the pad region and are thus free of any Ag pads (not shown in Fig. 1).
2. Al/nC: The cells feature a full area Al screen printing, but have pad regions without LCOs, i.e. no contacts (nC).
3. Ag/LCO: The cells have a screen printed Al rear side with Ag pads and LCOs also under the Ag pads.
4. Ag/nC: The cells are identical to group 3, but no LCOs are formed under the Ag pads.
5. Ag/nC BB: We also fabricate in the same batch solar cells with Ag pads located beneath the busbars (BB) and without LCOs in the pad region.

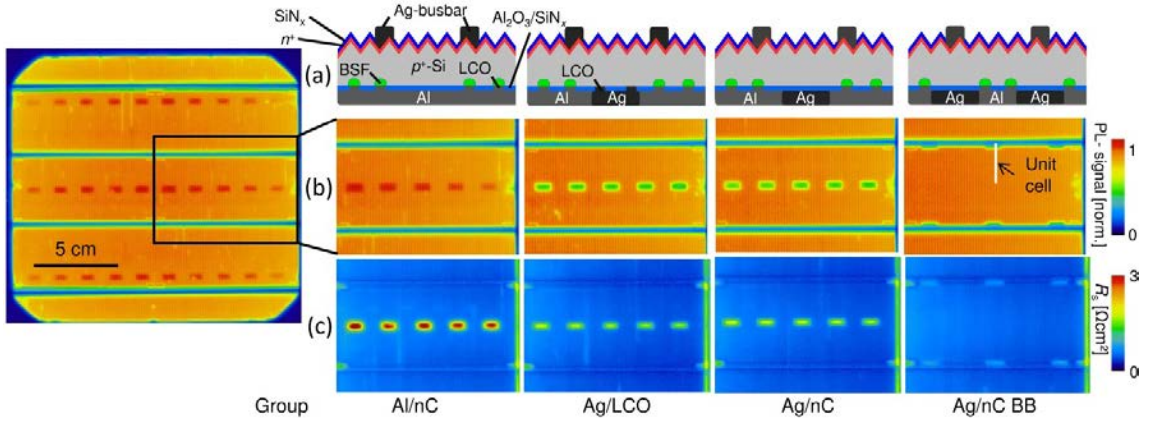

Fig. 1. Normalized PL-oc (b) and PL-R_S (c) images of solar cells fabricated with different combinations of LCOs and Ag pads. In group 2-4 the pads are located between the front side busbars to avoid their shading during measurements. Group 1 (no pads) featuring LCOs and Al screen printing on its full area, i.e. no pads, is not shown. The cross-sectional schematics (a) are not aligned to the orientation of the PL images. In the PL image of group 5 (Ag/nC BB) the white line indicates the unit cell of the simulations in section 3. The solar cells are designed to be cut into halves after processing.

For *IV*-testing we contact the front side busbar by contact pins that are equidistantly mounted to a bar (2.7 mm wide) and held in a frame. The type A uncertainty of the measurement device for PERC cells is for the efficiency η 0.04%$_{abs}$, for the short-circuit current J_{sc} 0.04mA/cm², for V_{oc} 0.1mV, and for the fill factor *FF* 0.13%$_{abs}$.Table 1 gives the IV-parameters of the cells of group 1-5. As observed in the PL images, the Ag paste (Ag/LCO and Ag/nC) increases the recombination, which reduces the V_{oc} by 4 mV. Regions without LCOs (Al/nC and Ag/nC) or with Ag pads (Ag/LCO and Ag/nC), where no Al BSF enables a base contact, increase the series resistance significantly from 0.41 Ωcm² (group 1) up to 0.60 Ωcm² as determined by the double-light method (DLM) at maximum power point (MPP) [9,10]. Since the determination of R_s includes various measurement uncertainties (J_{mpp} and V_{mpp} for two measurements), we additionally give the series resistance as determined by comparing the fill factor of the J_{sc}-V_{oc} and the IV-characteristics (R_s *FF*) [9,10]. The cells without pads have a series resistance of 0.47 Ωcm², whereas cells with pads have series resistances up to 0.61 Ωcm². LCOs above the Ag pads (Ag/LCO) have no influence on the V_{oc} as predicted in Ref. [5] and no significant effect on the series resistance, since no Ohmic contact is formed. Comparing the cells without Ag pads (Al/LCO) and the cells with pads under the busbar (Ag/nC BB) we observe a reduced effect on the V_{oc} and only a minor effect on the R_s since the pads are shaded.

Table 1. *IV*-parameters of solar cells with different pad configurations. 0 Ag pads corresponds to a full-area Al screen printing on the rear side. The values of group 1-4 are averages of three cells and group 5 of five cells.

Group	Number of Ag Pads	LCO above Pad	η [%]	J_{sc} [mA/cm²]	V_{oc} [mV]	*FF* [%]	R_s DLM [Ωcm²]	R_s *FF* [Ωcm²]
1 Al/LCO	0	Yes	20.27	38.41	659	80.12	0.41	0.47
2 Al/nC	0	No	20.17	38.44	659	79.66	0.57	0.55
3Ag/LCO	3×10 („between BB“)	Yes	19.78	38.26	655	78.95	0.57	0.59
4 Ag/nC	3×10 („between BB“)	No	19.84	38.39	655	78.93	0.60	0.61
5 Al/LCO BB	4×6 („under BB“)	No	20.09	38.37	657	79.64	0.44	0.47

3. Reducing the impact of the Ag pads

We observe that the Ag pads have an impact on the series resistance and on the open-circuit voltage. In order to minimize the latter effect we investigate an increased SiN_x thickness on the rear side. Therefore, we fabricate four different groups:

A: Ag/nC/100 nm: Cells with Ag pads between the busbars, no LCOs above the pads and a 100 nm SiN_x layer.
B: Ag/LCO/200 nm: Cells with Ag pads between the busbars having LCOs above the pads and a 200 nm SiN_x layer.
C: Ag/nC/200 nm: Cells with Ag pads between the busbars, no LCOs above the pads and a 200 nm SiN_x layer.
D: Al/nC/200 nm: Cells with pad regions without LCOs but Al screen printing, which are located between the busbars and a 200 nm SiN_x layer.

Figure 1 (b) shows the photoluminescence images taken at open-circuit voltage V_{oc} (PL-oc) of solar cells of group 2 through 5. The cells with Ag pads with and without LCOs (Ag/LCO and Ag/nC) have a reduced PL signal in the regions of the pads. This indicates that the Ag paste affects the dielectric layer and reduces the V_{oc} due to increased recombination. Above areas without LCOs and with Al (Al/nC) the PL signal is increased since these regions are free from LCOs and thus covered by a continuous passivation layer. There are no recombination active Si-metal contacts. The PL image of cells Ag/nC BB with the standard configuration having six pads under the busbars shows that the Ag pads are almost totally covered by the contact bars. Figure 1(c) shows the spatially resolved series resistance mapping based on luminescence images (PL-R_s) [8]. All solar cells show an increased series resistance in the pad regions, especially the cell Al/nC, where less recombination occurs. Due to the shading by the contact bars the effect is less pronounced for the cells Ag/nC BB.

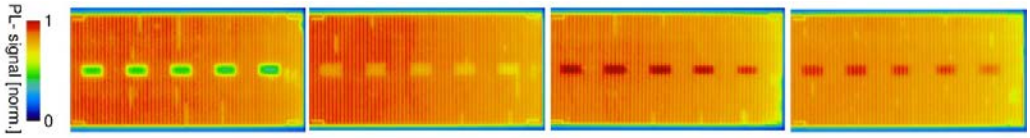

Group	A Ag/nC/100 nm	B Ag/LCO/200 nm	C Ag/nC/200 nm	D Al/nC/200 nm
Ag pads	yes	yes	yes	no
LCO above pads	no	yes	no	no
SiN_x thickness [nm]	100	200	200	200
V_{oc} [mV]	655	656	657	657

Fig. 2. Normalized PL-oc images of solar cells fabricated with different SiN_x layer thickness and combinations of LCOs and Ag pads. The images show the same close-up as in Fig. 1 and the pads are located between the front side busbars to avoid their shading during measurements. The open circuit values are averages of three cells each.

Since our hypothesis is that the elongated current path of the majority carriers causes the increase in series resistance, narrower Ag pads should reduce the series resistance contribution. We process one batch of solar cells and vary the pad thickness. Table 2 shows the resulting IV parameters of this batch. Comparing the cells without solder pads and the ones with the wide pads (w_p = 3.2 mm) shows a difference of R_s of 50 to 72 mΩcm². However, reducing the width of the pads to 2.1 mm, i.e., below the width of the measuring bars (2.7 mm), results in a comparable series resistance with respect to the solar cells without solder pads.

Table 2. *IV*-parameters of solar cells with different pad widths. 0 mm pad width w_p corresponds to cells without Ag pads. All values are averages for the group with w_p = 0 mm and 2.1 mm of 10 cells and for w_p = 3.2 mm of 9 cells.

w_p [mm]	η [%]	J_{sc} [mA/cm²]	V_{oc} [mV]	*FF* [%]	R_s DLM [Ωcm²]	R_s *FF* [Ωcm²]
0	20.5	39.3	654	79.8	0.554	0.563
2.1	20.4	39.2	654	79.4	0.539	0.588
3.2	20.2	39.2	652	79.1	0.605	0.636

4. Shading effects during cell measurements

During cell measurements contact bars, each with a shading width w_s of 2.7 mm contact the solar cells. We observed in the previous section for Ag pads with a width of 2.1 mm that there is no impact of the pads on the series resistance. One reason might be that due to the shading no charge carriers are generated above the pad and thus in this measurement configuration the pad has no impact on series resistance. Measuring a full cell with Kelvin contacts (two narrow contact needles, see Fig. 3), which do not shade the front side, is challenging due to series resistances in the contacts transporting the whole current of a large solar cell. Therefore, we laser cut cell pieces in the size of 30.8 × 7.5 mm² of solar cells processed as the ones in group 5, i.e, the Ag pads are located under the busbars. However, these cells have a 200 nm SiN_x instead of 100 nm, such that the open circuit voltage should be unaffected by enhanced recombination in the region of the Ag pads. These cell stripes are as wide as the distance between two busbars. The busbar is located in the center of the small cell. We choose the height similar as the height of the Ag pads, such that we have cells featuring an Ag pad on the whole busbar length. We measure 16 small cells that feature a pad on the rear side and 16 cells without solder pads. The cells are first measured using the contact frame with the 2.7-mm-wide contact bars, which shade the cell's front side. Since the small cells have a similar shading by the metal grid as the large cells, we use the same calibration as for the large cells, i.e., the light intensity is adjusted by an independently calibrated cell to match the cell current of an unshaded cell. Then, the cells are measured with the Kelvin contacts that avoid any shading, while keeping the short circuit current density for each cell constant with respect to the contact bar measurement. Therefore, we avoid any effects due to different current levels.

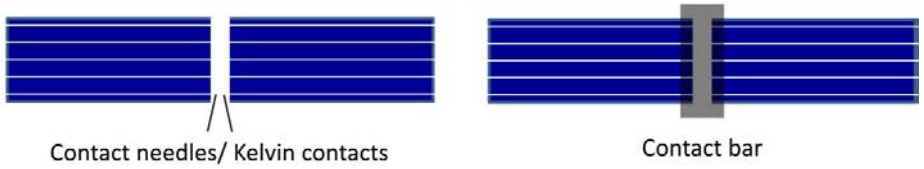

Fig. 3. Sketch of contact schemes: On the left side Kelvin contacts that do not shade the active cell are shown and on the right side the contact bar, which is much wider than the busbar is indicated.

Table 3. *IV*-parameters of cell pieces laser cut from large solar cells with and without Ag pad under the busbar. The given values are averages of 16 cells each. The cells are contacted by Kelvin contacts that do not shade the cell's front side or a contact bar shading 2.7 mm of the cell's front side.

Pad under busbar	Contacted by	η [%]	J_{sc} [mA/cm²]	V_{oc} [mV]	*FF* [%]	R_s DLM [Ωcm²]	R_s *FF* [Ωcm²]
no	Kelvin contacts	18.3	37.7	637	76.1	0.713	0.655
no	Contact bar	18.3	37.7	637	76.1	0.705	0.656
yes	Kelvin contacts	18.1	37.8	638	75.0	0.891	0.832
yes	Contact bar	18.2	37.8	638	75.4	0.795	0.746

Table 3 shows that for cells without Ag pad the measuring configuration has no significant impact on the series resistance or other cell parameters. However, the cells with an Ag pad show a significant increase in series resistance of about 90 mΩcm², when measured without shading compared to the case with the contact bar. This results in a reduction of the fill factor of 0.4%$_{abs}$. Comparing the measurements using the Kelvin contacts for the solar cells with and without Ag pads, we observe an increase in series resistance of 177 mΩcm², i.e. almost two times larger compared to the measurements with the contact bar. The measurements with the Kelvin contacts show a difference in fill factor for the cells with and without Ag pads of 1.1%$_{abs}$. Since the small cells are cut from the same large solar cells and from neighboring parts they show similar V_{oc} and J_{sc} values. However, due to the change in *FF* the efficiency is 0.2%$_{abs}$ lower.

5. Dependence of the series resistance on the front side shading width

In section three we observed that the proportion between the pad and the shading width has an impact on the strength of the series resistance due to an elongated current path. Therefore, we measure with Kelvin contacts and shade the front side by a black piece of paper with varying shading width w_s, see inset in Fig. 4. Again, we keep the short circuit current constant for all measurements. For the measurement of the cell without Ag pad we observe a linear increase in series resistance by the fill factor method (R_s *FF*). This increase in dependence of the shading width is caused by higher resistive power losses in the front metal grid, since the same current is generated at a larger distance from the busbar, where it is collected by the Kelvin contacts. The cell piece with Ag pad shows the same dependence for $w_s > 3.5$ mm > w_p, i.e. when the shading is wider than the pad. For $w_s < 3.5$ mm we observe a drastic increase in series resistance.

In order to verify the hypothesis that the increase in series resistance is caused due to the elongated current path for majority carriers, we perform numerical simulations using the conductive boundary model [11] as implemented in Quokka 2.2.4 [12]. The unit cell is 19.25 × 0.41 mm² in size, i.e., half the distance between two busbars times half the pitch of the rear contacts. We vary the shading width on the front side and focus on two cases: (i) the rear contact and the back surface field (BSF) is on the whole length of the unit cell corresponding to a cell without Ag pad ($w_p = 0$ mm) and (ii) the rear contact and the BSF are interrupted on a length of 1.6 mm to simulate an Ag pad with $w_p = 3.2$ mm.

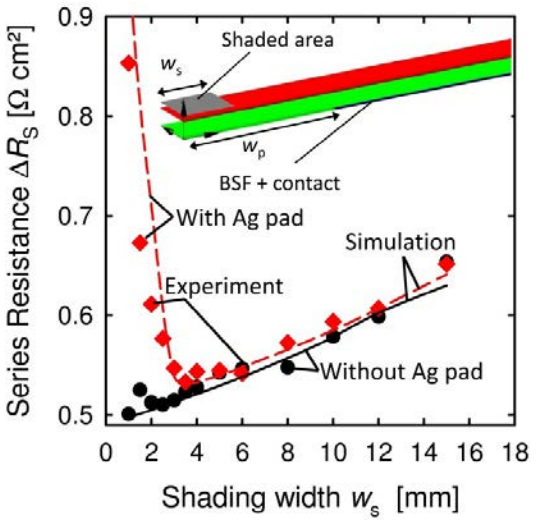

Fig. 4 Measured (symbols) and simulated (curves) series resistance R_s in dependence on the shading width w_s for cells without (black) and with Ag pads (w_p =3.2 mm, red). The inset shows a part of the unit cell indicating w_p and w_s.

We scale the light intensity depending on the shading width in order to keep the current constant for all simulations as in the experiments. The Quokka simulations include the increase in resistive losses in the emitter due to the increased current densities in the illuminated regions. The increase in series resistance in the fingers is calculated analytically assuming a finger resistance of 38.2 Ω/m [13]. To match the experimental data, the external series resistance is set for all simulations to 160 mΩcm², which is used as only free parameter.

Figure 4 shows the resulting simulated R_s extracted with the DLM as a function of the shading width w_s. The simulations without Ag pad reproduce the slope of the experimental values well and therefore the increase in series resistance with increased shading width can be explained by the increased emitter and finger resistive power losses. For $w_s > w_p$ the simulations for the cell with Ag pad show the same growth in series resistance as the cell with Ag pad. However, for $w_s < w_p$ R_s increases rapidly with decreasing shading width. Since effects in the emitter and the metallization are for both cases equal, we attribute the increase in series resistance for $w_s < w_p$ to the different transport in the bulk and in the back surface field. However, the BSF is as long as the contact region, therefore no significant transport is expected in the BSF. This leads us to the conclusion that the change in series resistance is caused by the majority carrier transport within the Si bulk above the Ag pad.

6. Conclusion

We observe two effects due to the application of Ag pads on PERC solar cells: (1) the decrease of the passivation quality of the dielectric layer between Ag and Si and (2) the increase of the series resistance due to an elongated current path for majority carriers generated above the pads. The first effect can be reduced by increasing the thickness of the passivation layer on the rear side from 100 nm to 200 nm SiN_x. Alternatively, Ag pastes that have less impact on the passivation quality may be used, even though the used paste is already a non-firing though paste.

On small-sized solar cells having Ag pads on the full length of the cell parallel to the busbar the second effect leads to an increase in series resistance of 177 mΩcm² and a difference in fill factor of 1.1%$_{abs}$. In case of a full-sized solar cells with only six pads the pads have in sum a length of 43.2 mm, which corresponds to 28% of the cell length. Scaling the fill factor loss by this 28% results in a decrease in *FF* of 0.3% $_{abs}$ and efficiency of 0.1% $_{abs}$. Depending on the pad configuration, e.g. 10 Ag pads per busbar, the effect can reach easily a decrease in efficiency of 0.2%$_{abs}$.

This effect can be omitted by reducing the pad width to the width of the front side shading as shown by the experiments and simulations. Thus, the pads should have a similar width as the ribbons used for interconnection to shade the pads. This avoids generation of charge carriers above the pads, which contribute to the lumped series resistance of the cell. The detection of the pad-induced R_s depends on the shading of the contact bar during *IV*-characterization and demands for improved contact concepts during measurements. In the final module the pads are shaded by the interconnector ribbons. If these are narrower than the contact bars, this results in an additional loss when comparing the cell tester results and the module performance.

Acknowledgement

The authors thank Ulrike Sonntag and Sarah Spätlich for cell processing as well as Bianca Lim, Martin Wolf, and Ingo Ahrens for support during cell characterization. The results were generated in the PERC2Module project funded by German Federal Ministry for Economic Affairs and Energy under Contract 0325641.

References

[1] SEMI Europe. *International Technology Roadmap for Photovoltaic (ITRPV) 2014 Results*. Available at: http://www.itrpv.net/.cm4all/iproc.php/Reports%20downloads/ITRPV_Roadmap_2015_Rev1_July_150722.pdf?cdp=a; 2015.

[2] Heimann M, Klaerner P, Luechinger C, Mette A, Mueller J, Traeger M, Barthel T, Valentin O, Wawer P. Ultrasonic Bonding of Aluminum Ribbons to Interconnect High-Efficiency Crystalline-Silicon Solar Cells. *Energy Procedia* 2012; **27**: 670–5, DOI: 10.1016/j.egypro.2012.07.127.

[3] Campe H von, Huber S, Meyer S, Reiff S, Vietor J. Direct tin-coating of the aluminum rear contact by ultrasonic soldering. In: *Proceedings of the 27th European Photovoltaic Solar Energy Conference and Exhibition*; 2012, pp. 1150–1153.

[4] Rotto NT, Meyer SR, Votava MJ, Meier DL. Cu Backside Busbar Tape: Eliminating Ag and Enabling Full Al Coverage in Crystalline Silicon Solar Cells and Modules. In: *Proceedings of the 42nd IEEE Photovoltaic Specialists Conference*; 2015, pp. in press.

[5] Kiefer F, Brendemühl T, Berger M, Lohse A, Kirstein S, Braun N, Lehr M, Heinemeyer F, Jung V, Morlier A, Blankemeyer S, Kunze I, Winter R, Harder N, Dullweber T, Köntges M, Brendel R. Influence of Solder Pads to PERC Solar Cells for Module Integration. *Energy Procedia* 2013; **38**: 368–74, DOI: 10.1016/j.egypro.2013.07.291.

[6] Reichel C, Granek F, Hermle M, Glunz SW. Investigation of electrical shading effects in back-contacted back-junction silicon solar cells using the two-dimensional charge collection probability and the reciprocity theorem. *J. Appl. Phys.* 2011; **109(2)**: 024507, DOI: 10.1063/1.3524506.

[7] Hannebauer H, Dullweber T, Baumann U, Falcon T, Brendel R. 21.2%-efficient fineline-printed PERC solar cell with 5 busbar front grid. *Phys. Status Solidi RRL* 2014; **8(8)**: 675–9, DOI: 10.1002/pssr.201409190.

[8] Trupke T, Pink E, Bardos RA, Abbott MD. Spatially resolved series resistance of silicon solar cells obtained from luminescence imaging. *Appl. Phys. Lett.* 2007; **90(9)**: 093506, DOI: 10.1063/1.2709630.

[9] Wolf M, Rauschenbach HS. Series resistance effects on solar cell measurements. *Advanced Energy Conversion* 1963; **3**: 455–79.

[10] Pysch D, Mette A, Glunz SW. A review and comparison of different methods to determine the series resistance of solar cells. *Solar Energy Materials and Solar Cells* 2007; **91(18)**: 1698–706, DOI: 10.1016/j.solmat.2007.05.026.

[11] Brendel R. Modeling solar cells with the dopant-diffused layers treated as conductive boundaries. *Prog. Photovolt: Res. Appl.* 2012; **20(1)**: 31–43, DOI: 10.1002/pip.954.

[12] Fell A, McIntosh KR, Abbott MD, Walter D. Quokka version 2: Selective surface doping, luminescence modeling and data fitting. In: *Proceedings of the 23rd International Photovoltaic Science and Engineering Conference 2013*; 2013.

[13] Witteck R, Hinken D, Schulte-Huxel H, Vogt MR, Muller J, Blankemeyer S, Kontges M, Bothe K, Brendel R. Optimized Interconnection of Passivated Emitter and Rear Cells by Experimentally Verified Modeling. *IEEE J. Photovoltaics* 2016; published online: 1–8, DOI: 10.1109/JPHOTOV.2016.2514706.